Department
of
APPLIED MATHEMATICS

On a Model for Continous Sedimentation in Vessels with Discontinously varying Cross-Sectional Area.

by

R. Bürger, K. H. Karlsen, N. H. Risebro, and J.D. Towers

Report no. 170 April 2002

UNIVERSITY OF BERGEN
Bergen, Norway

Department of Mathematics
University of Bergen
5008 Bergen
Norway

ISSN 0084-778X

On a Model for Continous Sedimentation in Vessels with Discontinously varying Cross-Sectional Area.

by

R. Bürger, K.H. Karlsen, N. H. Risebro and J. D. Towers

Report no. 170

April 2002

ON A MODEL FOR CONTINUOUS SEDIMENTATION IN VESSELS WITH DISCONTINUOUSLY VARYING CROSS-SECTIONAL AREA

R. BÜRGER, K. H. KARLSEN, N. H. RISEBRO, AND J. D. TOWERS

1. Mathematical model

In this paper, we study a clarifier-thickener configuration similar to that of our previous studies [4, 5, 6]. However, we now consider that the cross-sectional area of the settling vessel is not constant in both the clarification and the thickening zones.

We start by deriving in some detail the governing equation for continuous sedimentation in a vessel with varying cross section. In the formulation of the final initial value problem we add the feed source to the model for constant cross-sectional area formulated in [4, 5, 6].

We consider a segment of a vertical settling vessel with a variable cross-sectional area $S(x)$, where $-1 \le x \le 1$ is the dimensionless height variable. We let x increase downwards, and assume that $x = -1$ is the overflow level, $x = 0$ corresponds to the feed level and $x = 1$ is the discharge level. We assume that the unknown volumetric solids concentration u depends on height only, i.e., $u = u(x,t)$. Then the conservation of mass equation for the solids and the fluid is given by

$$S(x)u_t + \big(S(x)uv_{\mathrm{s}}\big)_x = 0, \tag{1}$$

$$-S(x)u_t + \big(S(x)(1-u)v_{\mathrm{f}}\big)_x = 0, \tag{2}$$

respectively, where t is time and v_{s} and v_{f} are the solids and the fluid phase velocities. The mixture flux, that is the volume average flow velocity weighted with $S(x)$, is given by

$$Q(x,t) := S(x)\big(uv_{\mathrm{s}} + (1-u)v_{\mathrm{f}}\big). \tag{3}$$

The sum of (1) and (2) produces the continuity equation of the mixture, $Q_x = 0$ for $-1 < x < 0$ and $0 \le x \le 1$ and $t > 0$, which implies that $Q(\cdot,t)$ is constant as a function of x. Since Q only suffers a jump across the feed source level $x = 0$, we get for $t > 0$

$$Q(x,t) = \begin{cases} Q(-1,t) = Q_{\mathrm{L}}(t) & \text{for } -1 \le x < 0, \\ Q(1,t) = Q_{\mathrm{R}}(t) & \text{for } 0 < x \le 1, \end{cases} \tag{4}$$

where $Q_{\mathrm{L}}(t) \le 0$ and $Q_{\mathrm{R}}(t) \ge 0$ are the signed volumetric suspension overflow and discharge rates, respectively, prescribed by the control of the suspension volume flows at $x = -1$ and $x = 1$. Note that we here identify a downwards flow with a flow to the right.

Equation (4) is equivalent to one of the mass balance equations. We let (4) replace (2) and rewrite (1) in terms of the flow rate $Q(x,t)$ and the solid-fluid relative velocity or slip velocity $v_{\mathrm{r}} := v_{\mathrm{s}} - v_{\mathrm{f}}$, for which a constitutive equation will be formulated. Observing that

$$uv_{\mathrm{s}} = \big(uv_{\mathrm{s}} + (1-u)v_{\mathrm{f}}\big)u + u(1-u)(v_{\mathrm{s}} - v_{\mathrm{f}}) = \frac{Q(x,t)u}{S(x)} + u(1-u)v_{\mathrm{r}},$$

and assuming for a moment that no solids enter the vessel at $x = 0$, we obtain from (1)

$$S(x)u_t + \big(Q(x,t)u + S(x)u(1-u)v_{\mathrm{r}}\big)_x = 0. \tag{5}$$

The well-known kinematic sedimentation theory [7, 12] is based on the assumption that v_{r} is a function of the local solids concentration u only, $v_{\mathrm{r}} = v_{\mathrm{r}}(u)$. We here express v_{r} in terms of the

The research was funded [in part] by the BeMatA program of the Research Council of Norway. We also acknowledge support by the Collaborative Research Program (Sonderforschungsbereich) 404 "Mehrfeldprobleme in der Kontinuumsmechanik" at the University of Stuttgart.

so-called Kynch batch flux density function h as $v_{\mathrm{r}}(u) = h(u)/(u(1-u))$, such that (5) takes the form

$$S(x)u_t + \big(Q(x,t)u + S(x)h(u)\big)_x = 0. \tag{6}$$

The function h is assumed to be piecewise differentiable with $h(u) = 0$ for $u \le 0$ or $u \ge u_{\max}$, where $u_{\max}$ is the maximum solids concentration, $h(u) > 0$ for $0 < u < u_{\max}$, $h'(0) > 0$ and $h'(u_{\max}) \le 0$. For simplicity we assume that (possibly after rescaling the problem) that $u_{\max} = 1$. A very frequently used function is due to Richardson and Zaki [13]:

$$h(u) = v_\infty u(1-u)^n, \quad v_\infty > 0,\ n \ge 1, \tag{7}$$

where $v_\infty > 0$ is the appropriately scaled settling velocity of a single particle in an unbounded pure fluid. For the analysis in this paper we will assume that $h \in C^2[0,1]$, and that h is genuinely nonlinear in the sense that $|h''| > 0$ except for finitely many inflection points.

Several authors have studied one-dimensional sedimentation in non-cylindrical vessels [1, 3, 8, 9, 15], using basically variants of (6), under the assumption that S is a smooth function of x. We are here interested in the analysis of (6) when S is only piecewise continuous, which means that the diameter jumps. In this case the available mathematical and numerical theory breaks down. The model studied here is very similar to problems of traffic flow with abruptly changing road conditions and of two-phase flow in porous media with jumps in permeability. We will assume that the cross section satisfies $S_{\min} \le S(x) \le S_{\max}$ for $x \in \mathbb{R}$ and $|S|_{BV} < \infty$, and that the initial data u_0 satisfies $u_0 \in L^1(\mathbf{R}) \bigcap BV(\mathbf{R})$, $0 \le u_0(x) \le 1$ for $x \in \mathbf{R}$.

To simplify the problem further, we assume $Q_{\mathrm{L}}(t) = Q_{\mathrm{L}} = \text{Const}$ and $Q_{\mathrm{R}}(t) = Q_{\mathrm{R}} = \text{Const}$. As in the clarifier-thickener setup studied in [4, 5], we assume that at $x = 1$, the composite solids flux $Q_{\mathrm{R}}u + S(x)h(u)$ is changed to the discharge transport flux $Q_{\mathrm{R}}u$, and that at $x = 0$, a feed source is located. To model this feed source, we recall that a clarifier-thickener unit with constant cross-sectional area S_0 can be modeled by the equation $u_t + \hat{g}(u,x)_x = 0$ with the composite flux

$$\hat{g}(u,x) = \begin{cases} q_{\mathrm{L}}u & \text{for } x < -1, \\ q_{\mathrm{L}}u + h(u) & \text{for } -1 < x < 0, \end{cases} \quad \begin{cases} q_{\mathrm{R}}u + h(u) + (q_{\mathrm{R}} - q_{\mathrm{L}})u_{\mathrm{F}} & \text{for } 0 < x < 1, \\ q_{\mathrm{R}}u + (q_{\mathrm{L}} - q_{\mathrm{R}})u_{\mathrm{F}} & \text{for } x > 1, \end{cases}$$

where $q_{\mathrm{L}} = Q_{\mathrm{L}}/S_0 \le 0$ and $q_{\mathrm{R}} = Q_{\mathrm{R}}/S_0 \ge 0$ are the prescribed volume overflow and discharge rates, respectively, divided by the cross-sectional area, and $u_{\mathrm{F}} \in [0, u_{\max}]$ is the concentration of the suspension fed into the unit through the singular source at $x = 0$ at the volumetric rate $Q_{\mathrm{F}} = Q_{\mathrm{R}} - Q_{\mathrm{L}}$. Subtracting the constant term $(q_{\mathrm{L}} - q_{\mathrm{R}})u_{\mathrm{F}}$ from the flux $\hat{g}(u,x)$ we obtain the equivalent conservation law $S(x)u_t + \tilde{g}(u,x)_x = 0$, where

$$\tilde{g}(u,x) = \begin{cases} Q_{\mathrm{L}}u + (Q_{\mathrm{L}} - Q_{\mathrm{R}})u_{\mathrm{F}} & \text{for } x < -1, \\ Q_{\mathrm{L}}u + S_0h(u) + (Q_{\mathrm{L}} - Q_{\mathrm{R}})u_{\mathrm{F}} & \text{for } -1 < x < 0, \end{cases} \quad \begin{cases} Q_{\mathrm{R}}u + S_0h(u) & \text{for } 0 < x < 1, \\ Q_{\mathrm{R}}u & \text{for } x > 1. \end{cases}$$

Finally, it is easy to see that we can state our problem of interest as the conservation law

$$S(x)u_t + g(u,x)_x = 0, \quad x \in \mathbb{R},\ t > 0, \tag{8}$$

$$g(u,x) = Q_{\mathrm{R}}u_{\mathrm{F}} + \begin{cases} Q_{\mathrm{L}}(u - u_{\mathrm{F}}) & \text{for } x < -1, \\ Q_{\mathrm{R}}(u - u_{\mathrm{F}}) & \text{for } x > 1, \end{cases} \quad \begin{cases} Q_{\mathrm{L}}(u - u_{\mathrm{F}}) + S(x)h(u) & \text{for } -1 < x < 0 \\ Q_{\mathrm{R}}(u - u_{\mathrm{F}}) + S(x)h(u) & \text{for } 0 < x < 1, \end{cases} \tag{9}$$

together with the initial condition

$$u(x,0) = u_0(x), \quad x \in \mathbb{R}; \quad u_0(x) \in [0, u_{\max}]\ \forall x. \tag{10}$$

A particular subcase included here is batch settling in a closed column. This occurs if we set $Q_{\mathrm{R}} = Q_{\mathrm{F}} = 0$ and hence $Q_{\mathrm{L}} = 0$. In this situation, we obtain the initial-value problem

$$S(x)u_t + g_{\mathrm{B}}(u,x)_x = 0, \quad x \in \mathbb{R},\ t > 0, \quad g_{\mathrm{B}}(u,x) = \begin{cases} 0 & \text{for } x < 0 \text{ and } x > 1, \\ S(x)h(u) & \text{for } 0 < x < 1. \end{cases} \tag{11}$$

Independently of the smoothness of the flux $g(u,\cdot)$ and the initial function u_0, solutions of (8)–(10) generally develop discontinuities, and so weak solutions must be sought. A *weak solution*

of the initial value problem (8)–(10) is a bounded function $u(x,t)$ satisfying, for all test functions $\phi \in \mathcal{D}(\mathbb{R} \times (0,T))$ with $\phi|_{t=T} = 0$,

$$\iint_{\Pi_T} \Big(S(x)u\phi_t + g(u,x)\phi_x \Big)\, dx\, dt + \int_{\mathbb{R}} S(x)u_0(x)\phi(x,0)\, dx = 0.$$

Our main result, whose proof appears in the next section, is stated in the following theorem:

Theorem 1. *There exists a weak solution to* (8)–(10), *and this weak solution can be constructed as a limit of a sequence of approximate solutions constructed by a finite difference scheme.*

2. Proof of Theorem 1

In order to facilitate the notation and analysis we now introduce the composite flux function $f(\boldsymbol{\gamma}(x), u) = g(u,x)$. Here $\boldsymbol{\gamma}(x) = (\gamma_1(x), \gamma_2(x))$ is the vector of flux parameters given by

$$\gamma_1(x) = S(x)\chi_{[-1,1]}(x), \quad \gamma_2(x) = \begin{cases} Q_{\mathrm{L}} & \text{for } x < 0, \\ Q_{\mathrm{R}} & \text{for } x > 0. \end{cases}$$

In this notation, the composite flux function is $f(\boldsymbol{\gamma}, u) = \gamma_2(u - u_{\mathrm{F}}) + \gamma_1 h(u) + Q_{\mathrm{R}} u_{\mathrm{F}}$. Thus the initial value problem for the conservation law (8) reads

$$S(x)u_t + f\big(\boldsymbol{\gamma}(x), u\big)_x = 0, \quad u(x,0) = u_0(x). \tag{12}$$

We now define a numerical method for (12). We choose a discretization Δx, set $x_j = j\Delta x$, and discretize the coefficient vector $\boldsymbol{\gamma}$, the initial data, and the cross sectional area by setting

$$\boldsymbol{\gamma}_{j+1/2} = \frac{1}{\Delta x}\int_{x_j}^{x_{j+1}} \boldsymbol{\gamma}(x)\, dx, \qquad U_j^0 = \frac{1}{\Delta x}\int_{x_{j-1/2}}^{x_{j+1/2}} u_0(x)\, dx, \quad S_j = \frac{1}{\Delta x}\int_{x_{j-1/2}}^{x_{j+1/2}} S(x)\, dx.$$

For $n > 0$ we define the approximations according to the explicit marching formula

$$U_j^{n+1} = U_j^n - \lambda_j \Delta_- f^{\mathrm{EO}}\left(\boldsymbol{\gamma}_{j+1/2}, U_{j+1}^n, U_j^n\right), \tag{13}$$

where $\lambda_j = \Delta t/(S_j \Delta x)$, $\Delta_- V_j = V_j - V_{j-1}$, and f^{EO} is the Engquist-Osher flux defined by

$$f^{\mathrm{EO}}(\boldsymbol{\gamma}, v, u) = \frac{1}{2}\left(f(\boldsymbol{\gamma}, u) + f(\boldsymbol{\gamma}, v) - \int_u^v |f_u(\boldsymbol{\gamma}, w)|\, dw \right). \tag{14}$$

Let $t_n = n\Delta t$ and let χ^n denote the characteristic function of $[t_n, t_{n+1})$ and χ_j the characteristic function of $[x_{j-\frac{1}{2}}, x_{j+\frac{1}{2}})$. We then define

$$u^\Delta(x,t) = \sum_{n\geq 0}\sum_j U_j^n \chi_j(x)\chi^n(t), \quad \text{and} \quad \boldsymbol{\gamma}^\Delta(x) = \sum_j \boldsymbol{\gamma}_{j+\frac{1}{2}}\chi_{j+\frac{1}{2}}(x).$$

The following lemma is easily established by a slight modification of arguments found in [6].

Lemma 1. *Let* $f_u^+(w) = \max(f_u(w), 0)$, $f_u^-(w) = \min(f_u(w), 0)$. *If the ratio* $\Delta x/\Delta t$ *is chosen so that the following CFL condition is satisfied*

$$\lambda_j \left| f_u^+(\boldsymbol{\gamma}_{j+\frac{1}{2}}, U_j^n) - f_u^-(\boldsymbol{\gamma}_{j-\frac{1}{2}}, U_j^n) \right| \leq 1, \quad \forall j \in \mathbf{Z}, \tag{15}$$

then the computed solutions remain in the interval $[0,1]$, *the CFL condition* (15) *holds for each succeeding time step, and the scheme* (13) *is monotone. In addition, there exists a constant* C, *independent of* Δ, *such that*

$$\sum_j \left| U_j^{n+1} - U_j^n \right| S_j \Delta x \leq \sum_j \left| U_j^1 - U_j^0 \right| S_j \Delta x \leq C\Delta t.$$

In what follows, we will use the Kružkov entropy-entropy flux pair indexed by c:

$$V(u) = |u - c|, \qquad F(\boldsymbol{\gamma}, u) = \operatorname{sign}(u - c)\big(f(\boldsymbol{\gamma}, u) - f(\boldsymbol{\gamma}, c)\big), \quad c \in \mathbb{R},$$

where $\operatorname{sign}(w) = w/|w|$ if $w \neq 0$ and $\operatorname{sign}(0) = 0$. We use the notation $\mathcal{O}\left(\Delta\boldsymbol{\gamma}_j\right)$ to denote terms which sum (over j) to $\mathcal{O}\left(|\boldsymbol{\gamma}|_{BV}\right)$. Furthermore, we use the notation Δ_+^u and Δ_-^u for spatial difference operators with respect to u only, keeping $\boldsymbol{\gamma}$ fixed, e.g.,

$$\Delta_+^u f(\boldsymbol{\gamma}_j, U_j^n) = f(\boldsymbol{\gamma}_j, U_{j+1}^n) - f(\boldsymbol{\gamma}_j, U_j^n) = \Delta_-^u f(\boldsymbol{\gamma}_j, U_{j+1}^n).$$

Similarly $\Delta_+^{\boldsymbol{\gamma}}$ and $\Delta_-^{\boldsymbol{\gamma}}$ denote spatial difference operators with respect to $\boldsymbol{\gamma}$ only with u kept fixed.

We now let $\chi^+(w;c)$ denote the characteristic function for the interval $[c, +\infty)$, $\chi^-(w;c)$ the characteristic function for $(-\infty, c]$. We will also use the notation $a_+ = \max(a, 0)$, $a_- = \min(a, 0)$. A proof of the following lemma can be found in [6].

Lemma 2. *For any constant $c \in \mathbb{R}$ and for all $j \in \mathbb{Z}$ the following inequalities hold:*

$$\pm\left(\int_{U_j^n}^{U_{j+1}^n} \chi^{\pm}(u;c) f_u^-\left(\boldsymbol{\gamma}_{j+\frac{1}{2}}, u\right) du + \int_{U_{j-1}^n}^{U_j^n} \chi^{\pm}(u;c) f_u^+\left(\boldsymbol{\gamma}_{j+\frac{1}{2}}, u\right) du\right) \leq \frac{\pm 1}{\lambda_j}\left(U_j^n - U_j^{n-1}\right)_{\pm} + \mathcal{O}\left(\Delta\gamma_j\right). \tag{16}$$

The following singular mapping will be used to transform the numerical approximations u^{Δ} into a sequence z^{Δ} for which compactness can be proved (see also [6] and the references therein):

$$\Psi(\boldsymbol{\gamma}, u) = \int_0^u |f_u(\boldsymbol{\gamma}, w)|\, dw. \tag{17}$$

Lemma 3. *For almost all $x \in \mathbb{R}$, the mapping $\Psi(\boldsymbol{\gamma}(x), u)$ is strictly increasing as a function of u, and $\Psi(\boldsymbol{\gamma}, u)$ is Lipschitz continuous with respect to u and $\boldsymbol{\gamma}$.*

Proof. From the definition of f, we see that $f_u(\boldsymbol{\gamma}(x), u) = \gamma_2(x) + \gamma_1(x) h_u(u)$. For $|x| > 1$, $f_u(\boldsymbol{\gamma}(x), u) = \gamma_2(x)$, which is nonzero because $Q_{\mathrm{L}} < 0$ and $Q_{\mathrm{R}} > 0$. For $x \in (0, 1)$, any zeros of $f_u(\boldsymbol{\gamma}(x), u)$ are isolated (in u), since $\gamma_1(x) > 0$ and h is genuinely nonlinear. This is also true for $x \in (-1, 0)$. That $\Psi(\boldsymbol{\gamma}(x), u)$ is strictly increasing is now immediate. For the Lipschitz continuity assertion, the following relationships are easily verified for $u \in [0, 1]$:

$$\big|\Psi(\boldsymbol{\gamma}, \tilde{u}) - \Psi(\boldsymbol{\gamma}, u)\big| \leq \|f_u\|\, |\tilde{u} - u|,$$
$$\big|\Psi(\tilde{\gamma}_1, \gamma_2, u) - \Psi(\gamma_1, \gamma_2, u)\big| \leq \|h_u\| |\tilde{\gamma}_1 - \gamma_1|, \quad \big|\Psi(\gamma_1, \tilde{\gamma}_2, u) - \Psi(\gamma_1, \gamma_2, u)\big| \leq |\tilde{\gamma}_2 - \gamma_2|.$$

□

Our goal at this point is to construct a certain decomposition of Ψ. Let $N_\epsilon(\mathbf{0})$ denote an open disk of radius ϵ centered at the origin in the γ_1-γ_2 plane, and define the set

$$\Gamma_\epsilon := \big([0, S_{\max}] \times [Q_{\mathrm{L}}, Q_{\mathrm{R}}]\big) \backslash N_\epsilon(\mathbf{0}).$$

Lemma 4. *There are finitely many functions $u_k^*(\boldsymbol{\gamma})$ such that*

$$0 = u_0^*(\boldsymbol{\gamma}) \leq u_1^*(\boldsymbol{\gamma}) \leq \cdots \leq u_{m-1}^*(\boldsymbol{\gamma}) \leq u_m^*(\boldsymbol{\gamma}) = 1,$$

and $|f_u(\cdot, \boldsymbol{\gamma})| > 0$ within each of the intervals $(u_k^*(\boldsymbol{\gamma}), u_{k+1}^*(\boldsymbol{\gamma}))$. In addition, each u_k^* depends Lipschitz continuously on the parameter vector $\boldsymbol{\gamma}$ in the sense that for any $\epsilon > 0$ there is a Lipschitz constant M_ϵ^k such that if

$$\text{the line segment joining } (\tilde{\gamma}_1, \tilde{\gamma}_2) \text{ to } (\gamma_1, \gamma_2) \text{ lies entirely within the set } \Gamma_\epsilon, \tag{18}$$

then

$$|u_k^*(\tilde{\gamma}_1, \tilde{\gamma}_2) - u_k^*(\gamma_1, \gamma_2)| \leq M_\epsilon^k\big(|\tilde{\gamma}_1 - \gamma_1| + |\tilde{\gamma}_2 - \gamma_2|\big). \tag{19}$$

Finally, for the discretized version of $\boldsymbol{\gamma}$, each adjacent pair of values $\boldsymbol{\gamma}_{j-\frac{1}{2}}$ and $\boldsymbol{\gamma}_{j+\frac{1}{2}}$ satisfies condition (18) with any value of ϵ for which $\epsilon < \min\big(-Q_{\mathrm{L}}, Q_{\mathrm{R}}, S_{\min}\big)$.

Proof. We start by observing that for fixed $\boldsymbol{\gamma}$ the critical points of $f(\boldsymbol{\gamma}, \cdot)$ satisfy the equation $\gamma_2 + \gamma_1 h_u(u) = 0$. We ignore for the moment the possibility that $\gamma_1 = 0$, which allows us to rewrite this as $-h_u(u) = \gamma_2/\gamma_1$. This makes it clear that for $\gamma_1 \neq 0$, the critical points of $f(\boldsymbol{\gamma}, u)$ (the solutions of $f_u(\boldsymbol{\gamma}, u) = 0$) are located in the u-z plane at the intersection of the graph of $z = -h_u(u)$ with the horizontal line $z = \gamma_2/\gamma_1$. For any single horizontal line of this type, there are only finitely many such intersections: this is a consequence of genuine nonlinearity.

In the u-z plane, we now construct a finite number of curves $\mathcal{C}_0, \ldots, \mathcal{C}_m$ as follows (the reader is urged to consult Figure 1 at this point): The curve $\mathcal{C}_0$ is just the vertical line $u = 0$. The definition of $\mathcal{C}_1$ starts with the portion of $z = -h_u(u)$ between $u = 0$ and the first turning point of $z = -h_u$. If the first turning point is a maximum (minimum), we continue the curve along the vertical half line lying above (below) the graph of $z = -h_u$. We also continue the curve $\mathcal{C}_1$ along the vertical line $u = 0$, choosing the upper half line or lower half line in such a way that z is always increasing or decreasing along $\mathcal{C}_1$. We then define $\mathcal{C}_2$ in a similar way, connecting the first and second critical points of $z = -h_u$, and then continuing the curve along vertical half lines consistent with the monotonicity of $z = -h_u$. Continuing this way, the final curve $\mathcal{C}_m$ will be the vertical line $u = 1$. By construction, a horizontal line of height z intersects each curve $\mathcal{C}_k$ exactly once. Let $v_k^*(z)$ denote the (unique) intersection at the curve $\mathcal{C}_k$. It is clear that each $v_k^*(z)$ is a Lipschitz continuous function of z, that $v_k^* \leq v_{k+1}^*$, and that each v_k^* is constant for $|z|$ sufficiently large. More specifically, there are constants $\underline{z}_k \leq \overline{z}_k$, and $v_k^*(-\infty)$, $v_k^*(+\infty)$ such that

$$v_k^*(z) = v_k^*(-\infty) \text{ for } z \leq \underline{z}_k, \quad v_k^*(z) = v_k^*(+\infty) \text{ for } z \geq \overline{z}_k.$$

Now recalling that $z = \gamma_2/\gamma_1$, we define

$$u_k^*(\boldsymbol{\gamma}) = \begin{cases} v_k^*(-\infty) & \text{for } \gamma_2 \leq \underline{z}_k \gamma_1, \\ v_k^*(\gamma_2/\gamma_1) & \text{for } \underline{z}_k \gamma_1 \leq \gamma_2 \leq \overline{z}_k \gamma_1, \\ v_k^*(+\infty) & \text{for } \gamma_2 \geq \overline{z}_k \gamma_1, \end{cases} \tag{20}$$

and observe that u_k^* is well-defined in the closed right half-plane $\{\boldsymbol{\gamma} | \gamma_1 \geq 0\}$, except possibly at the origin (due to differing radial limits). Moreover, if we exclude some neighborhood $N_\epsilon(\mathbf{0})$ of the origin, $u_k^*(\boldsymbol{\gamma})$ inherits Lipschitz continuity from $v_k(z)$. Indeed, given $\boldsymbol{\gamma}$ and $\tilde{\boldsymbol{\gamma}}$ such that the line segment connecting them lies in Γ_ϵ, if we integrate the gradient of u_k^* along that line segment, we get the Lipschitz estimate (19).

For each (relevant) value of $\boldsymbol{\gamma}$, define the following intervals, whose endpoints depend on $\boldsymbol{\gamma}$:

$$\mathcal{I}_k(\boldsymbol{\gamma}) = [u_k^*(\boldsymbol{\gamma}), u_{k+1}^*(\boldsymbol{\gamma})), \quad k = 0, \ldots, m-1,$$

By construction, the union of these intervals equals $[0, 1]$, and each of these intervals has Lipschitz continous length as long as the line segment joining the endpoints lies in Γ_ϵ. It is clear that by construction, there are no zeros of f_u in the interior of $\mathcal{I}_k$ (which may be empty), and so f_u is strictly monotone in the interior of $\mathcal{I}_k$.

We have only to check that $\boldsymbol{\gamma}_{j-\frac{1}{2}}$ and $\boldsymbol{\gamma}_{j+\frac{1}{2}}$ satisfy condition (18). Note first that we always have (with the notation $\boldsymbol{\gamma}_{j+\frac{1}{2}} = (\gamma_{j+\frac{1}{2},1}, \gamma_{j+\frac{1}{2},2})$) $Q_{\mathrm{L}} \leq \gamma_{j-\frac{1}{2},2} \leq Q_{\mathrm{R}}$ and $Q_{\mathrm{L}} \leq \gamma_{j+\frac{1}{2},2} \leq Q_{\mathrm{R}}$. If the intervals $I_{j-\frac{1}{2}}$ and $I_{j+\frac{1}{2}}$ lie entirely within $(-1, 1)$, then $S_{\min} \leq \gamma_{j-\frac{1}{2},1} \leq S_{\max}$ and $S_{\min} \leq \gamma_{j+\frac{1}{2},1} \leq S_{\max}$. Therefore, if $\epsilon < S_{\min}$, condition (18) is satisfied. If the intervals $I_{j-\frac{1}{2}}$ and $I_{j+\frac{1}{2}}$ lie entirely within $(-\infty, 0)$, then condition (18) is satisfied if $\epsilon < -Q_{\mathrm{L}}$. Similarly, if the intervals $I_{j-\frac{1}{2}}$ and $I_{j+\frac{1}{2}}$ lie entirely within $(0, \infty)$, then condition (18) is satisfied as long as $\epsilon < Q_{\mathrm{R}}$. Since any pair of intervals $I_{j-\frac{1}{2}}$, $I_{j+\frac{1}{2}}$ satisfies one of these three conditions, the proof is complete. □

Letting $\chi(w; \mathcal{I}(\boldsymbol{\gamma}))$ denote the characteristic function of the interval $\mathcal{I}(\boldsymbol{\gamma})$, we can now write down the decomposition of Ψ:

$$\Psi(\boldsymbol{\gamma}, u) = \int_0^u |f_u(\boldsymbol{\gamma}, w)| \, dw = \sum_{k=0}^{m} \int_0^u \chi(w; \mathcal{I}_k(\boldsymbol{\gamma})) \, |f_u(\boldsymbol{\gamma}, w)| \, dw =: \sum_{k=0}^{m} \Psi^k(\boldsymbol{\gamma}, u).$$

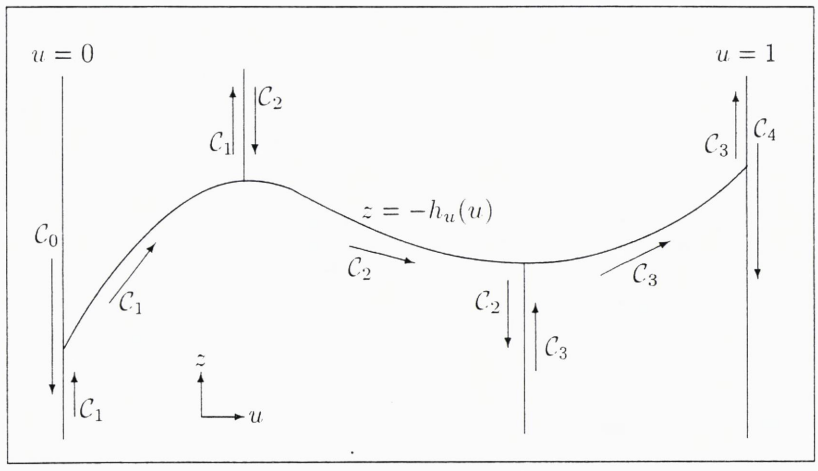

FIGURE 1. The curves $\mathcal{C}_k$ defined in the proof of Lemma 4. Any horizontal line $z =$ constant intersects each $\mathcal{C}_k$ exactly once.

Since f_u is Lipschitz continuous in γ, and the endpoints of each $\mathcal{I}_k(\tilde{\gamma})$ are Lipschitz continuous if condition (18) is satisfied, we have

$$\begin{aligned}\left|\Psi^k(\tilde{\gamma},u)-\Psi^k(\gamma,u)\right| \le \int_0^u &\left|\chi(w;\mathcal{I}_k(\tilde{\gamma}))-\chi(w;\mathcal{I}_k(\gamma))\right|\left|f_u(\tilde{\gamma},w)\right| \\ &+\chi(w;\mathcal{I}_k(\gamma))\left||f_u(\gamma,w)|-|f_u(\tilde{\gamma},w|\right| dw \le M\left|\tilde{\gamma}-\gamma\right|,\end{aligned}$$

for some constant M depending only on f, and hence Ψ^k is Lipschitz continuous in γ as long as condition (18) is satisfied.

For a fixed $i \in \{0,\cdots,m\}$, let P_+^i (N_+^i) denote those integers k, $0 \le i \le k \le m$, such that $f_u \ge 0$ (≤ 0) in the interval $\mathcal{I}_k$. Similarly, we let P_-^i (N_-^i) denote those integers k, $0 \le k < i \le m$, such that $f_u > 0$ (< 0) on $\mathcal{I}_k$. With these definitions, we can state the following lemma:

Lemma 5. *For each $i \in \{0,\cdots,M\}$ the following pair of inequalities holds:*

$$-\sum_{k\in N_+^i}\Delta_+^u\Psi^k\left(\gamma_{j+\frac{1}{2}},U_j^n\right)+\sum_{k\in P_+^i}\Delta_-^u\Psi^k\left(\gamma_{j-\frac{1}{2}},U_j^n\right)\le\frac{1}{\lambda_j}\left(U_j^n-U_j^{n+1}\right)_+ +\mathcal{O}\left(\Delta\gamma_j\right), \tag{21}$$

$$\sum_{k\in N_-^i}\Delta_+^u\Psi^k\left(\gamma_{j+\frac{1}{2}},U_{j+1}^n\right)-\sum_{k\in P_-^i}\Delta_-^u\Psi^k\left(\gamma_{j-\frac{1}{2}},U_j^n\right)\le-\frac{1}{\lambda_j}\left(U_j^n-U_j^{n+1}\right)_- +\mathcal{O}\left(\Delta\gamma_j\right). \tag{22}$$

Proof. Recalling that $\chi^+(u;u_i^*(\gamma_{j+\frac{1}{2}}))=0$ for $u<u_i^*(\gamma_{j+\frac{1}{2}})$ we find that

$$\begin{aligned}\int_{U_j^n}^{U_{j+1}^n}\chi^+(u;u_i^*\left(\gamma_{j+\frac{1}{2}}\right))f_u^-\left(\gamma_{j+\frac{1}{2}},u\right)du &=\sum_{k\in N_+^i}\int_{U_j^n}^{U_{j+1}^n}\chi(w;\mathcal{I}_k(\gamma_{j+\frac{1}{2}}))f_u^-\left(\gamma_{j+\frac{1}{2}},u\right)du \\ &=-\sum_{k\in N_+^i}\Delta_-^u\Psi^k\left(\gamma_{j+\frac{1}{2}},U_{j+1}^n\right).\end{aligned} \tag{23}$$

Similarly we find that

$$\int_{U_{j-1}^n}^{U_j^n}\chi^+(u;u_i^*\left(\gamma_{j+\frac{1}{2}}\right))f_u^+\left(\gamma_{j+\frac{1}{2}},u\right)du=\sum_{k\in P_+^i}\Delta_-^u\Psi^k\left(\gamma_{j+\frac{1}{2}},U_j^n\right), \tag{24}$$

$$\int_{U_j^n}^{U_{j+1}^n}\chi^-(u;u_i^*\left(\gamma_{j+\frac{1}{2}}\right))f_u^-\left(\gamma_{j+\frac{1}{2}},u\right)du=-\sum_{k\in N_-^i}\Delta_-^u\Psi^k\left(\gamma_{j+\frac{1}{2}},U_{j+1}^n\right), \tag{25}$$

$$\int_{U_{j-1}^n}^{U_j^n} \chi^-(u; u_i^*(\gamma_{j+\frac{1}{2}})) f_u^+(\gamma_{j+\frac{1}{2}}, u)\, du = \sum_{k \in P_-^i} \Delta_-^u \Psi^k(\gamma_{j+\frac{1}{2}}, U_j^n). \tag{26}$$

To conclude the proof we must replace the Δ^u difference operators by Δ operators. Recalling that Ψ^k is Lipschitz continuous in γ, we can replace $\gamma_{j+\frac{1}{2}}$ with $\gamma_{j-\frac{1}{2}}$ where required, absorbing the difference in the $\mathcal{O}(\Delta\gamma_j)$ term. Then we use (23) and (24) (with $\gamma_{j-\frac{1}{2}}$) in (16) (with $+$) and obtain (21). The inequality (22) is similarly obtained from (25), (26), and (16) (with $-$). □

Lemma 6. *For each $k = 0, \dots, m$, there exists a constant $C^k \geq 0$, independent of Δ and n, such that*

$$\sum_j \left|\Delta_+^u \Psi^k(\gamma_{j+\frac{1}{2}}, U_j^n)\right| \leq C^k. \tag{27}$$

Proof. From the definition of Ψ^k, and that $U_j^n \in [0,1]$, it follows that $|\Psi^k(\gamma_{j+\frac{1}{2}}, U_j^n)| \leq \|f_u\|$. Thus, for each $J > 0$

$$\left|\sum_{j=-J}^{J} \Delta_+ \Psi^k(\gamma_{j+\frac{1}{2}}, U_j^n)\right| \leq 2\|f_u\|, \tag{28}$$

$$\begin{aligned}
\sum_{j=-J}^{J} \left|\Delta_+^u \Psi^k(\gamma_{j+\frac{1}{2}}, U_j^n)\right| &= 2\sum_{j=-J}^{J} \left(\Delta_+^u \Psi^k(\gamma_{j+\frac{1}{2}}, U_j^n)\right)_+ - \sum_{j=-J}^{J} \Delta_+^u \Psi^k(\gamma_{j+\frac{1}{2}}, U_j^n) \\
&= 2\sum_{j=-J}^{J} \left(\Delta_+^u \Psi^k(\gamma_{j+\frac{1}{2}}, U_j^n)\right)_+ - \sum_{j=-J}^{J} \Delta_+ \Psi^k(\gamma_{j+\frac{1}{2}}, U_j^n) + \sum_{j=-J}^{J} \Delta_+^\gamma \Psi^k(\gamma_{j+\frac{1}{2}}, U_{j+1}^n) \\
&\leq 2\sum_{j=-J}^{J} \left(\Delta_+^u \Psi^k(\gamma_{j+\frac{1}{2}}, U_j^n)\right)_+ + 2\|f_u\| + \mathcal{O}(|\gamma|_{BV}).
\end{aligned} \tag{29}$$

Letting $J \to \infty$, we get

$$\sum_j \left|\Delta_+^u \Psi^k(\gamma_{j+\frac{1}{2}}, U_j^n)\right| \leq 2\sum_j \left(\Delta_+^u \Psi^k(\gamma_{j+\frac{1}{2}}, U_j^n)\right)_+ + 2\|f_u\| + \mathcal{O}(|\gamma|_{BV}).$$

Similarly, we find that

$$\sum_j \left|\Delta_+^u \Psi^k(\gamma_{j+\frac{1}{2}}, U_j^n)\right| \leq -2\sum_j \left(\Delta_+^u \Psi^k(\gamma_{j+\frac{1}{2}}, U_j^n)\right)_- + 2\|f_u\| + \mathcal{O}(|\gamma|_{BV}). \tag{30}$$

Without loss of generality, we can assume that $f_u > 0$ for $u \in I_0$. By this assumption $N_-^0 = \emptyset$ and $P_-^0 = \{0\}$, hence (22) with $i = 0$ reads

$$-\left(\Psi^0(\gamma_{j-\frac{1}{2}}, U_j^n) - \Psi^0(\gamma_{j-\frac{1}{2}}, U_{j-1}^n)\right) \leq -\frac{1}{\lambda_j}\left(U_j^n - U_j^{n+1}\right)_- + \mathcal{O}(\Delta\gamma_j).$$

Since the right hand side of this equation is nonnegative, it follows that

$$-\sum_j \left(\Delta_+^u \Psi^0(\gamma_{j+\frac{1}{2}}, U_j^n)\right)_- \leq \sum_j \frac{1}{\lambda_j}\left|U_j^1 - U_j^0\right| + \mathcal{O}(|\gamma|_{BV}).$$

Now using (30) produces the estimate

$$\sum_j \left|\Delta_+^u \Psi^0(\gamma_{j+\frac{1}{2}}, U_j^n)\right| \leq C^0 := 2\sum_j \frac{1}{\lambda_j}\left|U_j^1 - U_j^0\right| + \mathcal{O}(|\gamma|_{BV}).$$

Now we set $i = 2$ in (22), and recall that $P_-^1 = \{0\}$ and $N_-^1 = \{1\}$, in this case we find

$$\Delta_+^u \Psi^1(\gamma_{j+\frac{1}{2}}, U_j^n) + \Delta_+^u \Psi^0(\gamma_{j-\frac{1}{2}}, U_{j-1}^n) \leq -\frac{1}{\lambda_j}\left(U_j^n - U_{j-1}^n\right)_- + \mathcal{O}(\Delta\gamma_j).$$

Rearranging this, we see that

$$\sum_j \left(\Delta_+^u \Psi^1(\gamma_{j+\frac{1}{2}}, U_j^n)\right)_+ \leq \sum_j \left|\Delta_+^u \Psi^0(\gamma_{j+\frac{1}{2}}, U_j^n)\right| + \frac{-1}{\lambda_j}\left(U_j^n - U_{j-1}^n\right)_- + \mathcal{O}(\Delta\gamma_j),$$

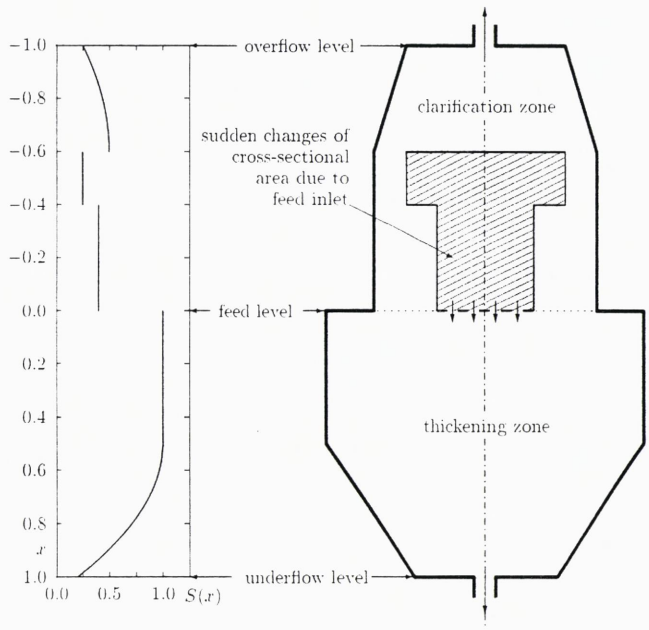

FIGURE 2. The function $S(x)$ used in the numerical examples and the vertical cross-section of a corresponding axisymmetric clarifier-thickener unit.

and thus by (29)

$$\sum_j \left|\Delta_+^u \Psi^1\left(\gamma_{j+\frac{1}{2}}, U_j^n\right)\right| \le 2C^0 + C^0 =: C^1.$$

Continuing inductively for $i = 2, 3, \ldots, m-1$, we see that

$$\sum_j \left|\Delta_+^u \Psi^i\left(\gamma_{j+\frac{1}{2}}, U_j^n\right)\right| \le 2\left(C^0 + C^1 + \cdots + E^{i-1}\right) + E^0 =: E^i.$$

For $i = m$, we use (21) and proceed as in the case where $i = 0$ to find that

$$\sum_j \left|\Delta_+^u \Psi^m\left(\gamma_{j+\frac{1}{2}}, U_j^n\right)\right| \le C^0 =: C^m.$$

□

Lettting now $z^\Delta = \Psi(\gamma^\Delta, u^\Delta)$, we have that

$$\left|z^\Delta(\cdot,t)\right|_{BV} = \sum_j \left|\Delta_+^u \Psi(\gamma_{j+\frac{1}{2}}, U_j^n)\right| + \left|\Delta_+^\gamma \Psi(\gamma_{j-\frac{1}{2}}, U_j^n)\right| \le \sum_{k=0}^{m} C^k + \mathcal{O}\left(|\gamma|_{BV}\right),$$

for all $t \ge 0$. Using this bound together with the obvious bounds,

$$\left|z^\Delta(x,t)\right| \le \max_{\gamma\in\Gamma} \Psi(\gamma, 1), \qquad \left\|z^\Delta(\cdot,t_1) - z^\Delta(\cdot,t_2)\right\|_{L^1(\mathbb{R})} \le C\left|t_1 - t_2\right|,$$

for some constant C independent of Δ. The second inequality, follows from Lemma 1, and the Lipschitz continuity of Ψ. By standard arguments, see, e.g., [11], it is straightforward to show that the sequence $\{u^\Delta\}_{\Delta>0}$ is compact in $L^1_{\mathrm{loc}}(\mathbb{R}\times\mathbb{R}^+)$. Let therefore $z = \lim_{\Delta\to 0} z^\Delta$ and define $u(x,t) = \Psi^{-1}(\gamma(x), z(x,t))$. Following [14], we can conclude that u is a weak solution of the initial value problem (12), and hence Theorem 1 follows.

3. NUMERICAL EXAMPLES

The physical problem and the finite difference scheme from Section 2 are now illustrated by some numerical examples. We assume that the function h is given by (7) with $v_\infty = 1$ and $n = 5$. The results are also valid for any other value $v_\infty > 0$ if the time variable is rescaled, and we

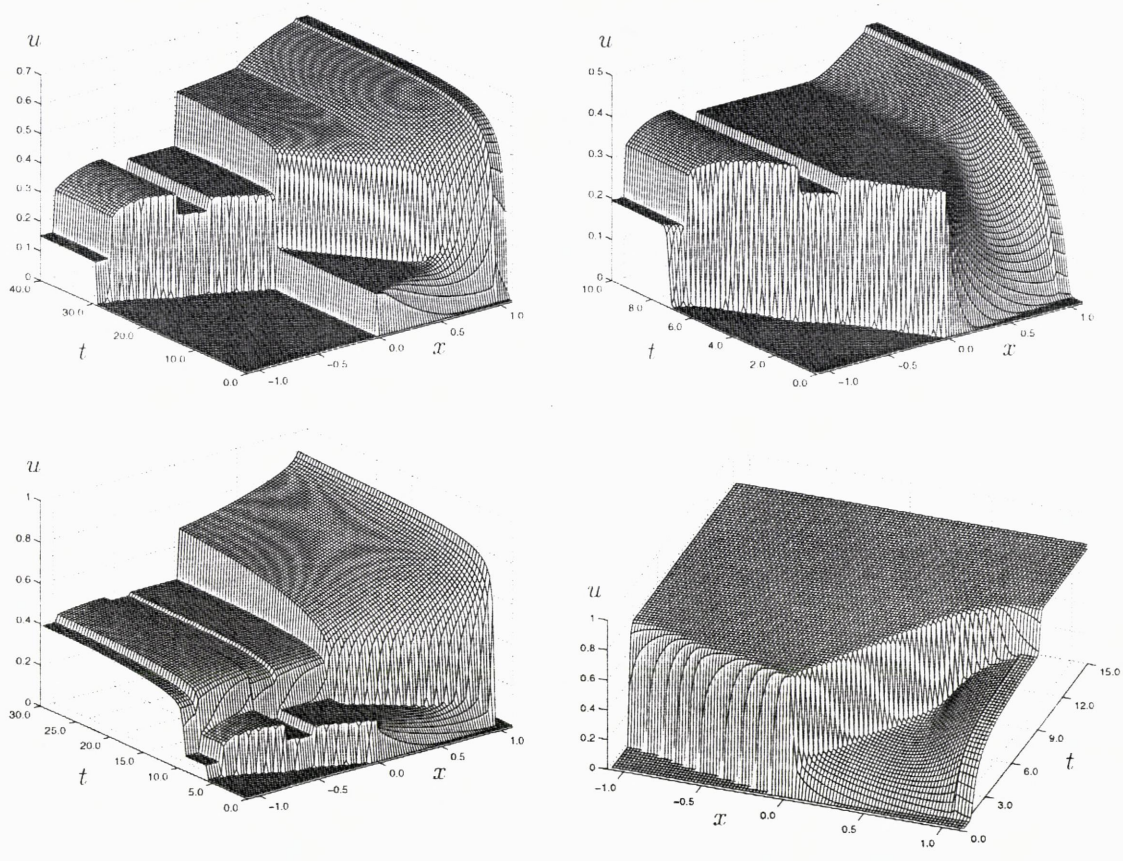

FIGURE 3. Simulation of the operation of the continuous clarifier-thickener at different operating conditions. Top left: Filling up the unit. Top right: Attaining steady state. Bottom left: Filling up the vessel at closed discharge. Bottom right: Hydraulic forcing with highly concentrated feed suspension.

mention that computations with this model function h (having the exponent $n = 5$) have also been presented in [2, 3].

Here, we let a clarifier-thickener unit be defined by the dimensionless function

$$S(x) = \begin{cases} 0.5 - 1.5625(x + 0.6)^2 & \text{for } x \in (-1, -0.6], \\ 0.25 & \text{for } x \in (-0.6, -0.4], \\ 0.5 & \text{for } x \in (-0.4, 0], \\ 1 & \text{for } x \in (0, 0.5], \\ 1 - 3.2(x - 0.5)^2 & \text{for } x \in (0.5, 1). \end{cases}$$

A vessel having this cross-sectional area function is sketched in Figure 2. The jumps of $S(x)$ are here caused by the shape of the vessel and by the space occupied by the interior feed mechanism.

In the numerical examples collected in Figure 3, we use $\Delta x = 1/100$ and $\lambda = 0.05$. Note that the computational grid is finer than the visual grid used to display the numerical results. The four cases considered here correspond to different choices of the parameters Q_{L}, Q_{R} and u_{F}, which are simply chosen as constants (with respect to time) and which lead to different modes of behaviour of the clarifier-thickener unit. For detailed analytical predictions of the clarifier-thickener response to operating conditions, we refer to [10] and the references cited in this paper.

The first case (top left plot) corresponds to $Q_{\mathrm{L}} = -0.1$, $Q_{\mathrm{R}} = 0.1$ and $u_{\mathrm{F}} = 0.4$. The simulation shows that the solids initially settle exclusively into the thickening zone ($x > 0$), accumulate there and form a rising sediment. This sediment layer breaks through the feed level ($x = 0$) at about $t = 20$ and the particles entering the clarification zone ($x < 0$) start to produce an overflow of clarified suspension at about $t = 29$. The shape of the concentration surface in the clarification zone reflects the vessel geometry, and that there the solution becomes stationary. Furthermore we see

that the concentration leaving the unit increases at $x = 1$ and decreases at $x = -1$ discontinuously. The system converges to a steady state of simultaneous clarification and thickening.

The second case (top right plot) is produced by the choice $Q_{\mathrm{L}} = -0.1$, $Q_{\mathrm{R}} = 0.4$ and $u_{\mathrm{F}} = 0.4$. This choice again leads to a stationary mode of operation, with the essential exception to the first case that the solids immediately start at $t = 0$ to enter the clarification zone.

The third case (bottom left plot) corresponds to $Q_{\mathrm{L}} = -0.2$, $Q_{\mathrm{R}} = 0.0$ and again $u_{\mathrm{F}} = 0.4$, i.e. the vessel is kept closed at its bottom. We observe that the thickening zone is slowly filled up. Moreover, as in the second example, particles start immediately to enter the clarification zone. However, an additional solids flux into the clarification zone is produced when the sediment rising in the thickening zone reaches the feed level. This leads to an increase of the concentrations in the clarification zone, which in contrast to the first and second case does not remain stationary.

The first three examples have in common that the solution at large times reflects the vessel geometry. This is not valid in the fourth case, where we apply an extreme feed flux by letting $Q_{\mathrm{L}} = -0.2$, $Q_{\mathrm{R}} = 0.2$ and $u_{\mathrm{F}} = 0.8$. In this situation, sometimes also called 'hydraulic forcing', the feed slurry immediately breaks into the clarification zone, which it leaves at its initial concentration. The thickening zone is first filled up successively, with a dilution of the feed suspension and sediment forming, but then is also filled up with the feed slurry at its feed concentration.

References

[1] Anestis, G., *Eine eindimensionale Theorie der Sedimentation in Absetzbehältern veränderlichen Querschnitts und in Zentrifugen*, Doctoral Thesis, Technical University of Vienna, Austria, 1981.

[2] Bürger, R. and Concha, F. (2001) 'Settling velocities of particulate systems: 12. Batch centrifugation of flocculated suspensions', *Int. J. Mineral Process.* **63** (2001), 115–145.

[3] Bürger, R., Damasceno, J.J.R. and Karlsen, K.H., 'A mathematical model for batch and continuous thickening in vessels with varying cross section', Preprint, University of Bergen/Preprint 2001/11, SFB 404, University of Stuttgart.

[4] Bürger, R., Karlsen, K.H., Klingenberg, C. and Risebro, N.H., 'A front tracking approach to a model of continuous sedimentation in ideal clarifier-thickener units', *Nonlin. Anal. Ser. B: Real World Appl.*, to appear.

[5] Bürger, R., Karlsen, K.H., Risebro, N.H. and Towers, J.D., 'Numerical methods for the simulation of continuous sedimentation in ideal clarifier-thickener units'. Preprint, University of Bergen/Preprint 2001/10, SFB 404, University of Stuttgart.

[6] Bürger, R., Karlsen, K.H., Risebro, N.H. and Towers, J.D., 'Convergence of a difference scheme for continuous sedimentation in ideal clarifier-thickener units'. In preparation.

[7] Bustos, M.C., Concha, F., Bürger, R. and Tory, E.M., *Sedimentation and Thickening.* Kluwer Academic Publishers, Dordrecht, The Netherlands, 1999.

[8] Chancelier, J.P., Cohen de Lara, M., Joannis, C. and Pacard, F., 'New insights in dynamic modeling of a secondary settler—I. Flux theory and steady-states analysis', *Wat. Res.* **31** (1997), 1847–1856.

[9] Diehl, S., 'Dynamic and steady-state behavior of continuous sedimentation', *SIAM J. Appl. Math.* **57** (1997), 991–1018.

[10] Diehl, S., 'Operating charts for continuous sedimentation I: Control of steady states', *J. Eng. Math.* **41** (2001), 117–144.

[11] H. Holden and N.H. Risebro, *Front tracking for conservation laws.*, Springer Verlag, New York, to appear.

[12] Kynch, G.J., 'A theory of sedimentation', *Trans. Faraday Soc.* **48** (1952), 166–176.

[13] Richardson, J.F. and Zaki, W.N., 'Sedimentation and fluidization: Part I.', *Trans. Instn. Chem. Engrs. (London)* **32** (1954), 35–53.

[14] Towers, J.D., 'A difference scheme for conservation laws with a discontinuous flux - the nonconvex case, SIAM J. Numer. Anal. **39** (2001), 1197–1218.

[15] White, D.A. and Verdone, N., 'Numerical modelling of sedimentation processes', *Chem. Eng. Sci.* **55** (2000), 2213–2222.

(Bürger)
INSTITUTE OF MATHEMATICS A, UNIVERSITY OF STUTTGART
PFAFFENWALDRING 57, D-70569 STUTTGART, GERMANY.
E-mail address: buerger@mathematik.uni-stuttgart.de

(Karlsen)
DEPARTMENT OF MATHEMATICS, UNIVERSITY OF BERGEN
JOHS. BRUNSGT. 12, N–5008 BERGEN, NORWAY
E-mail address: kennethk@math.uib.no

(Risebro)
DEPARTMENT OF MATHEMATICS, UNIVERSITY OF OSLO
P.O. BOX 1053. BLINDERN, N–0316 OSLO, NORWAY
E-mail address: nilshr@math.uio.no

(Towers)
MIRACOSTA COLLEGE, 3333 MANCHESTER AVENUE
CARDIFF-BY-THE-SEA, CA 92007-1516, USA
E-mail address: jtowers@cts.com